Theor Appl Climatol
DOI 10.1007/s00704-014-1306-9

ORIGINAL PAPER

Snow cover variations in Gansu, China, from 2002 to 2013

Xun Liu · Chang-Qing Ke · Zhu-De Shao

Received: 7 April 2014 / Accepted: 19 October 2014

Abstract Gansu is an inland province located in the northwest of China with an arid to semi-arid climate and a developed animal husbandry. Snowmelt in Gansu is an important source of water for rivers and plays an important role in ecological environment and social-economic activities. In this study, Moderate Resolution Imaging Spectroradiometer (MODIS) 8-day composite snow products MOD10A2 and MYD10A2 are combined to analyse snow cover variations during the snow season (October to March) period from 2002 to 2013. We define the snow area percentage (SAP) and snow cover occurrence percentage (SCOP) to analyse the spatial and temporal characteristics of the snow cover variation in Gansu. In addition, we apply the Mann-Kendall test to verify the SAP inter-annual variation. The results indicate that the SAP in Gansu remained above 5 % with three peaks in November, December and January. SAP varies a lot in the four sub-regions of Gansu, with the highest in the Gannan Plateau sub-region and the lowest in the Longzhong Loess Plateau sub-region in most of the snow seasons examined. The SCOP is high in the southwest mountains and low in the northeast Gobi and desert. The SCOP is highly related to elevation in most of Gansu, with an exception in the high mountains. In the Hexi Desert and oasis region, the SAP significantly decreases during the snow season, particularly in February and March. We find that there are a significantly negative correlation between SCOP and temperature during the snow season and a significantly positive correlation between SCOP and precipitation in December.

X. Liu · C.-Q. Ke (✉) · Z.-D. Shao
Jiangsu Provincial Key Laboratory of Geographic Information Science and Technology, Key Laboratory for Satellite Mapping Technology and Applications of State Administration of Surveying, Mapping and Geoinformation of China, Collaborative Innovation Center of Novel Software Technology and Industrialization, Nanjing University, No. 163 Xianlin Avenue, 210023 Nanjing, China
e-mail: kecq@nju.edu.cn

X. Liu
e-mail: sumor2014@163.com

Z.-D. Shao
e-mail: shaozd2007@126.com

1 Introduction

Snow cover is an important component of the cryosphere and reaches 46 million km^2 during the winter in the Northern Hemisphere (Frei and Robinson 1999). On a global scale, snow cover has a high reflectivity, which makes it a significant component in a climate system. Also, it affects energy balance and atmospheric circulation through a series of complicated interactions and feedback mechanisms (Barnett et al. 1988; Cohen and Rind 1991). Moreover, snow cover is a sensitive indicator of climate change and can quickly respond to global warming (Linde and Grab 2011; Bavay et al. 2009). On a regional scale, snowmelt is an important water resource for arid and semi-arid regions (Shi et al. 2007). However, excessive snow due to snowstorms can affect agriculture development, animal husbandry and resident lives and property (Wang et al. 2013). During the spring, fast-rising temperature can cause extreme hydrological disasters such as floods and debris flow because of snowmelt. Monitoring snow cover and analysing its spatial and temporal variations on different scales have been a hot topic of study worldwide (Liang et al. 2008).

The traditional method for monitoring snow cover was to use in situ snow depth data from meteorological stations. However, the spatial distribution of the meteorological stations in west China is sparse. In situ data can only determine whether snow is present or not at the meteorological stations and cannot provide the spatial distribution of the snow cover in a sparse station network (Pu et al. 2007). Remote sensing techniques have been applied for monitoring snow cover for more than 40 years, and a series of snow cover algorithms and

Published online: 30 October 2014

products has been developed (Dewey and Heim 1982; Ramsay 1998; Hall et al. 2002; Grody and Basist 1996). Microwave (e.g. SMMR, SSM/I and AMSR-E) and optical sensors (e.g. AVHRR, Landsat, SPOT and Moderate Resolution Imaging Spectroradiometer (MODIS)) have been widely used to monitor snow cover (Frei and Robinson 1999; Ke et al. 2009; Armstrong and Brodzik 2001; Bulygina et al. 2011; Maskey et al. 2011; Foppa and Seiz 2012; Mazari et al. 2013; Ke and Liu 2014). In 1999, the National Aeronautics and Space Administration (NASA) launched the Terra satellite, with on-board MODIS sensor, providing MODIS snow cover products (MOD10) through a series of algorithms (Hall and Riggs 2007). Due to its free availability, appropriate resolution and high accuracy, MODIS snow cover products have been used as the main remote sensing data for spatial and temporal snow cover studies (Zhou et al. 2005). Recently, Tang et al. (2013) used the MOD10A1 product to examine the temporal and spatial variations of snow cover across the Tibetan Plateau from 2001 to 2011. Maskey et al. (2011) applied the MOD10A2 product and temperature data to compare the temporal and spatial snow cover variations in the Himalayas from 2000 to 2008. Pu and Xu (2009) applied the MOD10C2 product to analyse the factors that influence snow cover fraction (SCF), such as slope, aspect and surface curvature in the Tibetan Plateau from 2000 to 2006. In addition, Liang et al. (2008) applied the MOD10A1 and MOD10A2 products to monitor snow cover of pastures in the northern Xinjiang and compared the differences between the two products.

Gansu Province is a typical arid and pastoral area in northwest China with widely distributed snow cover during the snow season. However, Gansu faces serious desertification and soil erosion problems (Luo et al. 2005). Snowmelt from the Qilian and Animaqing mountains is an important source of water for river runoff. Moreover, Gansu is the main animal husbandry farming area in China. Large area and long duration of snow can cause considerable disasters and husbandry losses. Han et al. (2011) used NOAA and MODIS data to analyse the spatial and temporal distributions of snow cover from 1997 to 2006 in the Qilian Mountains. They found that the snow cover area decreased in the east and middle portion of the mountains and increased in the west portion. In this paper, we apply data from the MODIS 8-day composite snow product to analyse the spatial and temporal distributions of snow cover in the entire Gansu and to further explore the relationships between snow cover variations and climate and elevation factors.

2 Study area and data

2.1 Study area

Gansu Province is located in northwest China between latitudes of 32° and 43° N and longitudes of 92° and 103° E, covering a total area of 453,700 km^2. The terrain is higher in the southwest than in the northeast. Gansu is a narrow (narrowest distance of less than 100 km) but long extension of about 1500 km from the westernmost edge to the easternmost edge (Fig. 1). Gansu is usually divided into four subregions based on landscape and climate differences: Longzhong Loess Plateau region, Longnan mountainous region, Gannan Plateau region and Hexi Desert and oasis region (Feng 1989). The Longzhong Loess Plateau region is located in the middle-east of Gansu Province, the western part of the Loess Plateau, with an annual mean precipitation of 200–600 mm. The Longnan mountainous region is a transition zone among the Tibetan Plateau, Loess Plateau and Sichuan Basin, with an elevation of 2000–4000 m and an annual precipitation of 400–1000 mm. The Gannan Plateau region is in the eastern margin of the Tibetan Plateau and is part of the water source of the Yellow River, with an elevation generally exceeding 3000 m. The Hexi Desert and oasis area is dominated by deserts and mountains, including the Hexi Corridor area, Bei Mountains to the northwest and Qilian Mountains to the south. In particular, Qilian Mountain region in Gansu accounts for the most abundant snow resource. In this region, ice and snowmelt serve as the water source for three river systems (Ejina River, Shiyang River and Shule River), including 56 inland rivers (Han et al. 2011).

2.2 MOD10A2 and MYD10A2

The NASA Earth Observing System (EOS) Terra and Aqua satellites were launched in 1999 and 2002, respectively, and were equipped with MODIS sensors. These MODIS sensors can be used to fully observe ecosystems on Earth and provide a variety of data products, such as the snow product, which is mainly generated from a SNOMAP algorithm (Hall et al. 1995). The EOS-Terra MOD10A2 and EOS-Aqua MYD10A2 are both snow cover products. MOD10A2 is a composite of the daily MOD10A1 data and shows the maximum range of snow cover over 8 days. Specifically, if a pixel is marked as snow for any of the 8 days in MOD10A1, the corresponding pixel of MOD10A2 is identified as snow (Xie et al. 2009). If no snow is observed, the MOD10A2 marks the pixel as no snow. If clouds appear on any of the 8 days, the pixel is identified as clouds. Different pixel values represent the following different ground objects: 25 for no snow cover, 37 for lakes, 50 for cloud, 100 for lake ice and 200 for snow cover. Because there is minimal snow in the summer, the study is conducted during snow seasons only (from October to March of 2002–2013). The data are downloaded from the National Snow and Ice Data Centre (NSIDC) website. The MODIS Reprojection Tool (MRT) provided by the NSIDC is used to process the MODIS snow products, including merging images and converting sinusoidal projections to the Universal Transverse Mercator (UTM) projection. The spatial resolution

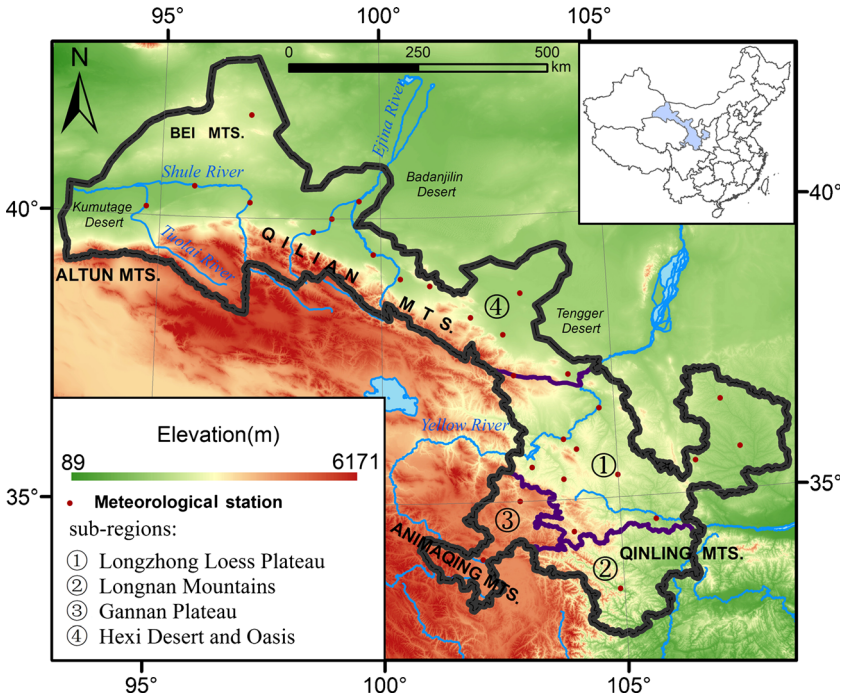

Fig. 1 The study area: Gansu Province and its four sub-regions and available weather stations

is resampled to 500 m. Finally, the images are cropped to only include the area under the Gansu provincial administrative boundary.

The accuracy of the MODIS 8-day snow data was verified previously (Zhou et al. 2005). Wang et al. (2008) compared the MOD10A2 with in situ snow depth data and found that the accuracy of the MOD10A2 reached 94 % at snow depths ≥4 cm on cloud-free days. Huang et al. (2007) found that the average MOD10A2 accuracy in the northern Xinjiang was up to 87.5 %. Although Hall and Riggs (2007) suggested that the MOD10A2 error is relatively large when the snow depth is less than 1 cm, recognition accuracy is generally high, indicating that MOD10A2 can be used to monitor snow cover and its variations and trends.

2.3 Shuttle Radar Topography Mission digital elevation model data

The Shuttle Radar Topography Mission (SRTM) is a NASA mission conducted in 2000 to obtain elevation data for most of the world. It is the current dataset of choice for digital elevation model data (DEM) since it has a fairly high resolution (about 90 m at the equator and <30 m in the USA) and has near-global coverage (from 56° S to 60° N). SRTM DEM has been publicly released in 2003 and revised many times. Data used for the study is version 4.1 (Farr et al. 2007). To match the MODIS snow product, we resample the SRTM DEM at a resolution of 500 m to provide a relevant snow cover distribution and elevation analysis.

2.4 In situ data

The temperature, precipitation and snow depth data at 29 weather stations in Gansu are obtained from China Meteorological Data Sharing Service System (http://cdc.cma.gov.cn). The distribution of the meteorological stations is uneven, with most of them in the Longzhong Loess Plateau region. Only a few of them are located in the mountain areas, e.g. Wushaoling Station is located at a relatively high elevation. There is no meteorological station in the Qilian Mountains, which are the main snow cover distribution areas in Gansu (Fig. 1).

3 Method

3.1 Combination of MOD10A2 and MYD10A2

In the presence of clouds, the optical sensors cannot see through the clouds to map the ground surface. Thus, clouds are a considerable obstacle when monitoring snow cover by MODIS. Compared to the daily snow data of MOD10A1 and MYD10A1, MOD10A2 and MYD10A2 have 8-day temporal resolution while with much less cloud coverage due to the 8-day combination of daily products (Zhou et al. 2005). Currently, most cloud removal algorithms are applied to daily data (Parajka et al. 2010; Xie et al. 2009; Paudel and Andersen 2011). For the 8-day data, the cloud removal approach combined MOD10A2 and MYD10A2 as MODMYD (Liang et al. 2008). MYD10A2 is similar to MOD10A2 although the

failure of band 6 in MODIS Aqua. Because snow has a strong absorption band at 2.1 μm, band 6 is replaced with band 7 to calculate the NDSI. In this case, the data accuracy is not considerably affected (Salomonson and Appel 2006). On certain days, the EOS-Terra satellite passes overhead in the morning and the EOS-Aqua satellite passes overhead in the afternoon. Although snow cover is relatively stable, a dynamic change of cloud often occurs between morning and afternoon. This is the principle of removing cloud cover to reveal snow cover after combining MOD10A2 and MYD10A2. Figure 2 shows examples of reducing cloud cover and revealing snow cover. After combination, the cloud coverage of MODMYD is overall reduced by half as compared with either MOD10A2 or MYD10A2. Therefore, more snow cover is revealed and snow cover percentage is increased (Table 1).

3.2 Snow area percentage and snow cover occurrence percentage calculations

The snow area percentage (SAP) is calculated as the percentage of the number of pixels identified as snow over the total number of pixels of the study area. During a given period, the amount of MODMYD images is fixed. For each pixel, the percentage that snow appears in the pixel over the total MODMYD images is defined as snow cover occurrence percentage (SCOP) of the pixel (Eq. 1). If snow cover occurs in the pixel for all MODMYD images, then SCOP=100 %. If there is no snow in the pixel for all MODMYD images, then SCOP=0 %. A higher SCOP value indicates that the pixel is covered by snow for a longer time during the given period.

$$\mathrm{SCOP}(a) = \frac{T_{\mathrm{snow}}}{T} \times 100\% \tag{1}$$

where a represents the given period, for a pixel, T_{snow} represents the counts that the pixel is identified as snow and T represents the number of MODMYD images during the given period. We calculate the SCOP values for the annual snow season and for each month.

3.3 Mann-Kendall test

A non-parametric rank-based Mann-Kendall test is often used to test the variation trends in hydrological and meteorological time series, such as river runoff, temperature, precipitation and sea ice (Sönmez et al. 2014; Oguntunde et al. 2006; Biggs and Atkinson 2011; Xia et al. 2014). This test can be applied to data that are not normally distributed. The statistical value of the Mann-Kendall test, S, is calculated according to Eq. 2:

$$\mathrm{S} = \sum_{k=1}^{n-1} \sum_{j=1}^{n} \mathrm{Sgn}\left(x_j - x_k\right) \tag{2}$$

where x_j and x_k are the SAP at different times, and x_j occurs later than x_k. Sgn( ) is the sign function. When $x_j - x_k$ is smaller than, equal to or greater than 0, $\mathrm{Sgn}(x_j - x_k)$ is −1, 0 or 1, respectively. In addition, n represents the total number of MODMYD images in a given period of time. When the Mann-Kendall statistical value of S is greater than, equal to or smaller than 0, the following Eq. 3 holds:

$$\begin{cases} Z = \dfrac{S-1}{\sqrt{\dfrac{n(n-1)(2n+5)}{18}}} \\ Z = 0 \\ Z = \dfrac{S+1}{\sqrt{\dfrac{n(n-1)(2n+5)}{18}}} \end{cases} \tag{3}$$

A positive value of Z indicates an increasing trend, and a negative value for a decreasing trend. When the absolute value of Z is greater than or equal to 1.28 or 1.64, significance levels of 90 and 95 %, respectively, are satisfied. We apply the Mann-Kendall test to examine the variation trends of the SAP in Gansu and the four sub-regions.

4 Results

4.1 Monthly SAP variations

During the snow seasons, the mean SAP of 12 years (2002–2013) in the entire Gansu remains above 5 % (Fig. 3, top). From October to mid-November, the SAP continues to increase. When the SAP peaks (20.3 %) in mid-November, it remains relatively stable but gradually increases to 23.4 % in mid-January and then gradually decreases to 6.5 % by the end of March. There are three peaks in the SAP curve during the snow season because Gansu is a main region in China with variable snow coverage. In contrast with areas with stable snow coverage, such as Xinjiang or northeast China, many areas do not have stable snow coverage that remains through the entire winter. Instead, accumulation and melting processes occur intermittently throughout the winter. In addition, snow area is affected by unexpected weather, which results in unpredictable timing for the maximum SAP every year (which can appear from November to January).

Figure 3 (bottom) also shows the snow area variations in the four sub-regions. In the Gannan Plateau regions, snow accumulation occurs relatively early and snowmelt occurs relatively late. In October, November, February and March, the SAP is much greater in this region than that in the other regions. The highest SAP reaches 34.6 % in November. In December, the snow area significantly decreases over a short

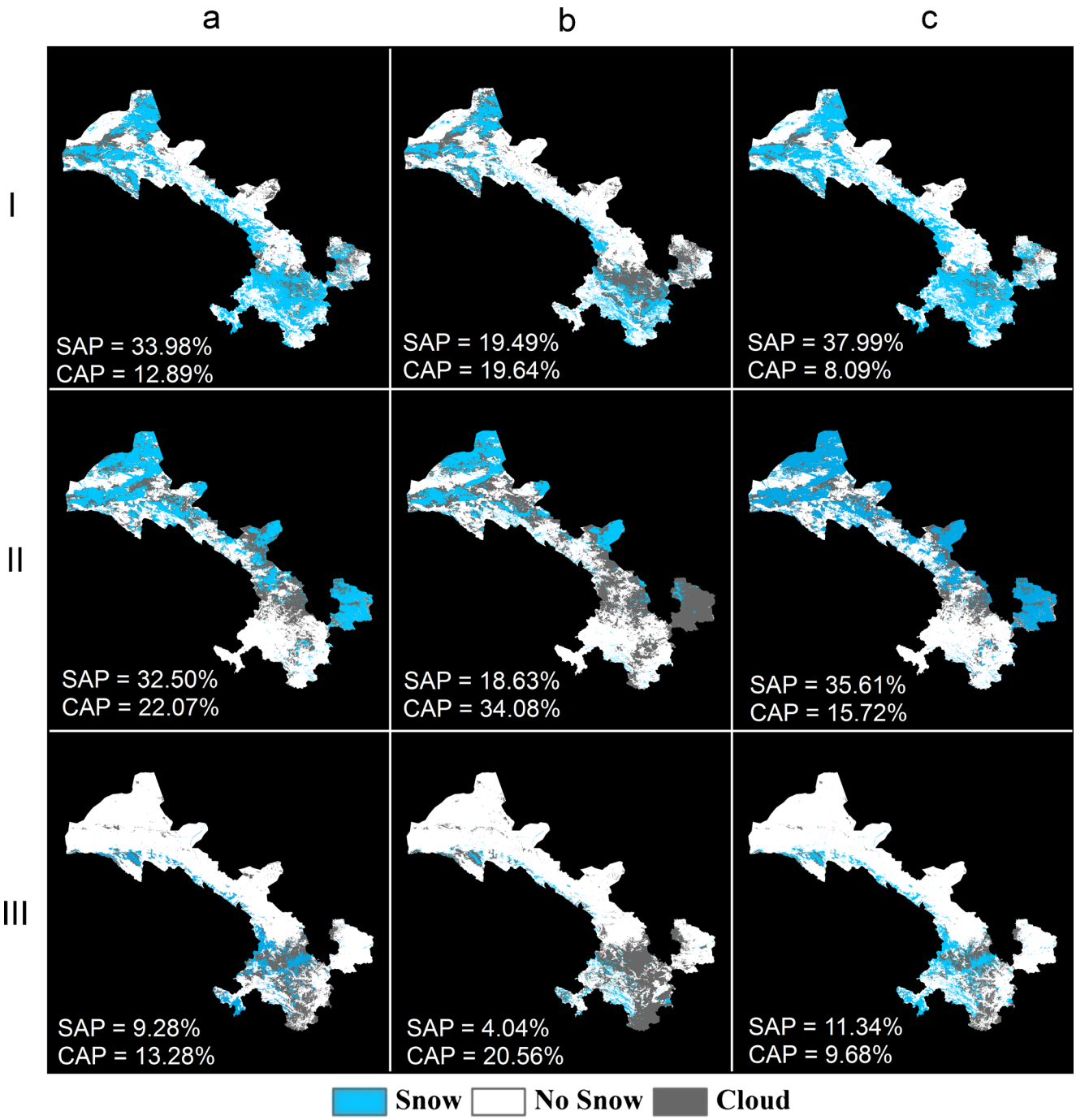

Fig. 2 Examples showing combination of MOD10A2 and MYD10A2 in reducing cloud area percentage (*CAP*) and revealing more snow area percentage (*SAP*). *Top panel* (*I*): 27 December 2004–3 January 2005, *middle panel* (*II*): 17 January 2006–25 January 2006, *bottom panel* (*III*): 10 February 2012–17 February 2012, *left panel* (*a*): MOD10A2, *middle panel* (*b*): MYD10A2 and *right panel* (*c*): MODMYD

Table 1 Area change of cloud and snow after combining MOD10A2 and MYD10A2

	MOD10A2 (%)	MYD10A2 (%)	MODMYD (%)
Average CAP	4.71	5.68	2.79
Average SAP	11.21	9.47	13.93

CAP cloud area percentage, *SAP* snow area percentage

time, which indicates that the snow area variations in the Gannan Plateau could be related to the snow cover characteristics of the Tibetan Plateau (i.e. the snow area in the winter is smaller than that in the spring or fall) (Tang et al. 2013). The elevation of Longzhong Loess Plateau region is relatively low while concentrated with the most populations and cities in Gansu. This area has the smallest snow area percentage, with the highest snow cover (up to 18.9 %) occurring in late

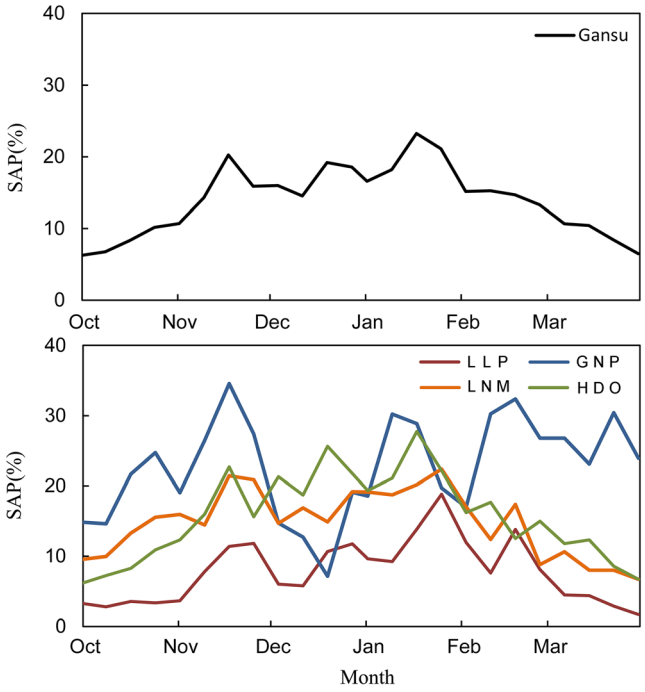

Fig. 3 Time series mean snow area percentage (*SAP*) during the snow seasons from 2002 to 2013 for the entire study area (*top*) and each sub-region (*bottom*). *LLP* Longzhong Loess Plateau region, *LNM* Longnan mountainous region, *GNP* Gannan Plateau region, *HDO* Hexi Desert and oasis region

January. In the Longnan Mountains and Hexi Desert and oasis areas, the SAP variation is similar. In October, the SAP is relatively high in the Longnan mountainous area. In December and January, the SAP is relatively high in the Hexi Desert and oasis area, with the maximum value exceeding 20 %.

4.2 Monthly SCOP variations

During the snow season, the areas with the highest SCOP values are mainly distributed in the Qilian Mountains (Fig. 4). However, because the Qilian Mountains are composed of many parallel mountains and valleys, the terrain is complicated. In this region, the higher mountains are covered by snow throughout the snow season. In the mountains at the border of the Qinghai and Gansu provinces, the SCOP exceeds 80 %. In the transition zone from Qilian Mountains to Hexi Corridor, the elevation is approximately 2000 m and the SCOP reaches 50 %. However, in the broad valley between the parallel Qilian Mountains, although the elevation is relatively high, the SCOP is low. For example, in the Tuolai River valley in the northern section of the Qilian Mountains, the SCOP is approximately 30 % during the winter. In addition, the SCOP is relatively low in the part of the Kumutage Desert that is located in the broad valley of the Qilian Mountains and the Altun Mountains.

The SCOP during the winter is relatively high at other areas in Gansu, such as Bei Mountains, which is located at the border between northern Gansu and Mongolia. The snow season occurs between November and February each year. Here, the SCOP is highest in December. For the Animaqing Mountains in the Gannan Plateau region and Minshan Mountains in the Longnan mountainous region, SCOP values are the largest in the spring, followed in the fall and then in the winter. In particular, the SCOP values are the highest in March, especially apparent in the Animaqing Mountains. SCOP variations are consistent with the regulation of intra-annual snow cover variations on the Tibetan Plateau. The Ejina River Valley in northern Gansu is a narrow channel with high SCOP between the Great Gobi and Badanjilin deserts of Inner Mongolia.

The SCOP values in Gansu gradually decline from the southwest to the northeast. In most areas, the highest SCOP values are in January, with an exception that the peak SCOP in the Gannan Plateau region occurs in March. The SCOP in some areas, such as the Kumutage Desert (borders the Xinjiang in northwest Gansu) and the edge of the Tengger Desert (in the northern Longzhong Loess Plateau), remains low in January with deficient water resources. The aforementioned Tuolai River valley between the parallel Qilian Mountains has low SCOP values.

4.3 Inter-annual SAP variations

Table 2 shows the Mann-Kendall trend analysis results. Although the study period is relatively short, a significant decreasing trend (at 95 % significance level) is found in the Hexi Desert and oasis region in February and March, as well as in the entire snow season. There are many deserts in this region that may be subjected to desertification and soil erosion from changing snowmelt. A significant reduction in spring snow coverage could result in reduced river streamflow and intensified desertification. A weak increasing trend (at 90 % significance level) is found in December and in the entire snow season for the Longnan mountainous region. A similar weak increasing trend also occurred in October and January for the Longzhong Loess Plateau region and in October for the Gannan Plateau region. No apparent variation trends occurred in the other regions during the other months (Table 2).

5 Discussion

5.1 The relationships between SCOP and elevation

Generally, more snow coverage occurs at higher elevations. However, the relationships between the snow coverage and elevation are complicated. To analyse this relationship, we presume that elevation and SCOP are correlated linearly and

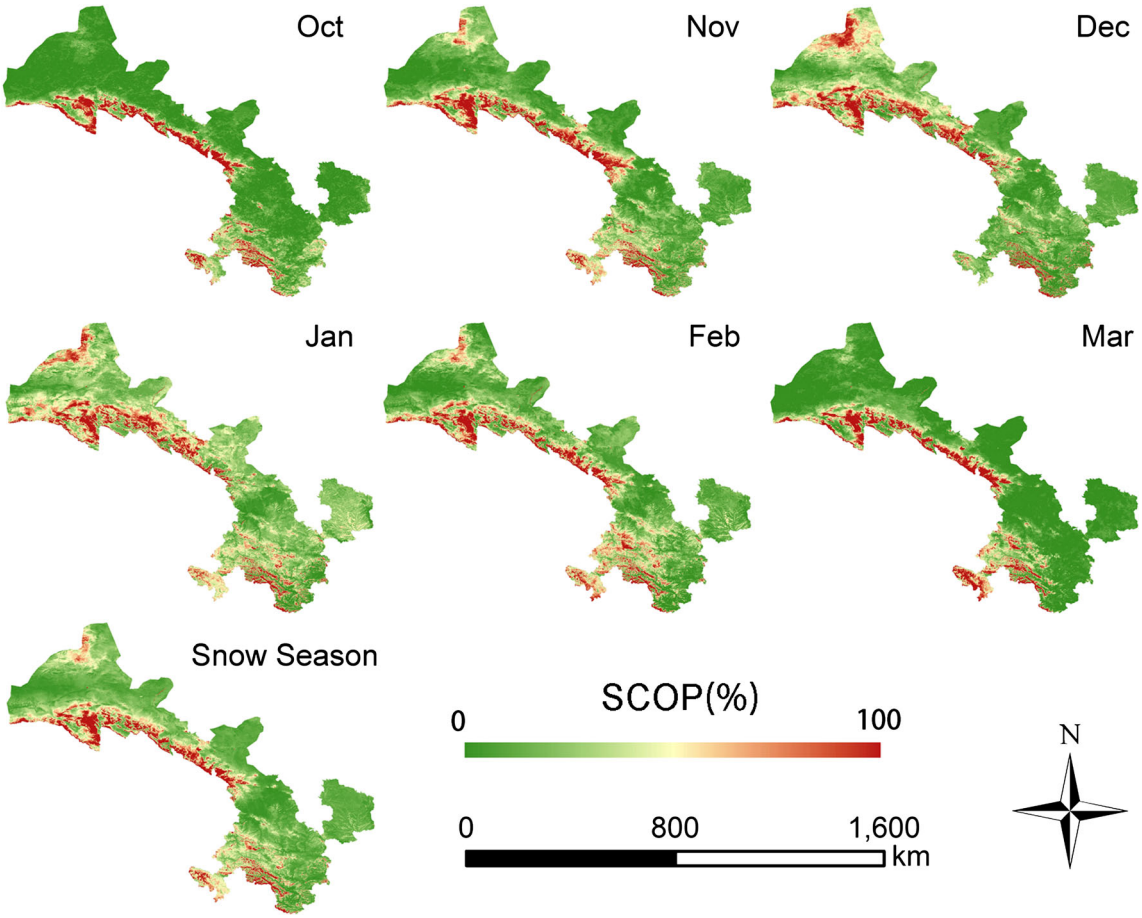

Fig. 4 Spatial distribution of snow cover occurrence percentage (*SCOP*) during the snow seasons (October to March) and each month

positively during the snow season. We calculate the approximate relationship between elevation and SCOP. In this case, pixels with greater elevation correspond to greater SCOP value. Thus, elevation and SCOP are correlated linearly and positively. We define the normalised snow-elevation correlation index (NSECI) as follows:

$$\mathrm{NSECI} = 1 - \mathrm{abs}\left[(\mathrm{SCOP} - \mathrm{SCOP}_{\min}) \Big/ (\mathrm{SCOP}_{\max} - \mathrm{SCOP}_{\min}) - (H - H_{\min}) \Big/ (H_{\max} - H_{\min})\right] \quad (4)$$

where the SCOP represents the total SCOP for the snow seasons in Gansu and H is the elevation. We initially derive the dimensionless values for both SCOP and elevation by using the normalised deviation method to represent the ranking percentages and their respective value ranges (between 0 and 1). Next, we subtract the absolute value of their difference from 1. If their ranking percentages are similar, the NSECI is close to 1. This result indicates a large SCOP and a very high elevation or a very small SCOP and a very low elevation. Conversely, if their ranking percentage is significantly different, the NSECI is close to 0. Pixels with high NSECI index indicate that elevation substantially affects the snow cover distribution. In contrast, a location with a low NSECI index indicates that other factors rather than elevation affect the snow cover distribution. We calculate the NSECI index for Gansu and divide it into five levels: extremely low correlation (0–0.4), low correlation (0.4–0.6), moderate correlation (0.6–0.8), high correlation (0.8–0.9) and extremely high correlation (>0.9). The area percentages are 0.12, 4.84, 26.48, 39.28 and 29.29 % for the extremely low, low, moderate, high and extremely high correlations, respectively (Fig. 5). Therefore, in most areas, SCOP and elevation are highly correlated. The area with a NSECI index of more than 0.8 accounts for approximately 70 % of the total area, while the area with a NSECI index of more than 0.6 accounts for approximately 95 % of the total area. Furthermore, regions with low NSECI values indicate that the snow cover is determined by the local terrain and topography. In the aforementioned wide valley of the Qilian Mountains, the SCOP is low; however, the elevation at this location exceeds 3500 m.

Table 2 Mann-Kendall trend test of SAP in the four sub-regions and the entire Gansu

	GNP	HDO	LLP	LNM	Gansu
October	+	NST	+	NST	NST
November	NST	NST	NST	NST	NST
December	NST	NST	NST	+	NST
January	+	NST	NST	NST	NST
February	NST	−	NST	NST	NST
March	NST	−	NST	NST	NST
ESS	NST	−	NST	+	NST

+ increasing trend at 90 % significance level, − decreasing trend at 95 % significance level, *NST* no significant trend, *ESS* entire snow seasons, *GNP* Gannan Plateau region, *HDO* Hexi Desert and oasis region, *LLP* Longzhong Loess Plateau region, *LNM* Longnan mountainous region

The models for calculating the relationships between the NSECI and elevation are relatively simple. In fact, the relationships between elevation and snow cover are much more complicated than a linear correlation. Elevation is not the only one factor that affects the snow cover distribution. Furthermore, some regional terrain and topography (such as mountains and valleys) affect the snow cover distribution especially in high-elevation regions. Therefore, the NSECI is more appropriate for relatively low-elevation areas. However, by using NSECI, we can approximately reveal the relationships between elevation and snow cover distribution in Gansu.

5.2 Relationship between SCOP and meteorological factors

We extract the SCOPs from the pixels of 29 weather stations in Gansu. If SCOP is greater than 0, we compute correlation coefficients between SCOP and the monthly average temperature, amount of precipitation and snow depth at the weather station. During the snow seasons (Table 3), a strong negative correlation ($r=-0.7$) occurred between temperature and SCOP. The correlation coefficient in all months, except January, exceeds −0.6, all at 95 % significance level.

Correlation coefficients between precipitation and SCOP are all positive although relatively small. However, it is significant in December at 95 % significance level and nearly significant in January and February. This is because precipitation in these 3 months should be mostly snowfall. In other months, however, rainfall could occur and could actually reduce snow cover. No correlation is found between the snow depth and SCOP because Gansu is a region of unstable snow coverage. Thus, the main climate factor that controls snow cover in Gansu is temperature, while precipitation has some influence on the SCOP from December to February.

6 Conclusions

The cloud cover area is reduced by 40 % when the MODIS 8-day snow data products, MOD10A2 and MYD10A2, are combined into MODMYD. By using MODMYD for the snow seasons from 2002 to 2013, we examine the temporal and spatial variations of the SAP and SCOP for snow cover in Gansu. In situ observation data is also used to explore the relationships between SCOP and temperature and precipitation.

During the snow season, the SAP in Gansu exceeds 5 %. The snow accumulation period occurs from early October

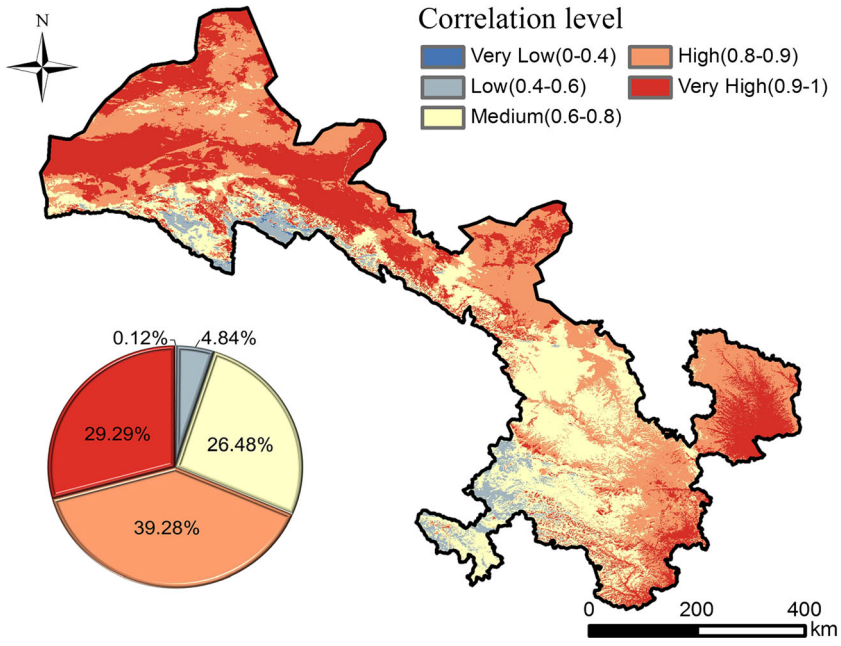

Fig. 5 Normalised snow-elevation correlation index (NSECI) in Gansu from 2002 to 2013 (the *pie chart* represents the proportion of each correlation level)

Table 3 Relationship between SCOP and temperature, precipitation and snow depth

	Temperature	Precipitation	Snow depth
October	*−0.64*	0.09	0.15
November	*−0.66*	0.03	−0.08
December	*−0.66*	*0.47*	0.28
January	*−0.53*	0.35	0.09
February	*−0.68*	0.36	0.08
March	*−0.73*	0.20	0.15
ESS	*−0.70*	−0.07	0.17

Numbers in italics indicate 95 % significance level

ESS entire snow seasons

through the middle of November, and the stable period of snow cover occurs from late November to late January. The ablation period of snow cover occurs from late January to the end of March. Among the four sub-regions, temporal and spatial snow cover variations in the Gannan Plateau region are similar to those in the Tibetan Plateau. The SAP values are greater in fall and spring than those in winter with relatively larger SAP fluctuations. The SAP is the lowest in the Longzhong Loess Plateau area. Because there are many mountains in the southern Gansu and the Hexi Desert and oasis area, the seasonal variations in the SAP are similar. In Gansu, the areas with the highest SCOPs are the Qilian Mountains (except for some gullies in the Qilian Mountains), Bei Mountains, the Animaqing Mountains and the western region of the Qinling Mountains. Areas with relatively low SCOPs include the valleys in the Qilian Mountains, the Hexi Desert and oasis and the Gobi Desert areas. In most regions, the SCOP is the highest in January. However, in the Gannan Plateau region, the SCOP is the highest in March.

During the snow seasons, the SAP in the Hexi Desert and oasis region significantly decreases, which is particularly obvious in February and March. This decrease most likely reduces inland river runoff and exacerbates desertification in the Hexi region. Because the time series is relatively short, most of the other regions did not display significant SAP variation trends. In most areas, a strong correlation exists between SCOP and elevation. However, the correlation between SCOP and elevation in the Qilian Mountains is relatively weak, and the snow cover in the Qilian Mountains is determined by the local terrain and topography. A strong negative correlation occurs between SCOP and temperature, and a relatively strong and positive correlation occurs between precipitation and SCOP in December.

Although the MOD10A2 and MYD10A2 products were combined, an average of 2 % cloud cover occurred in each image scene, which resulted in a slight underestimation of snow cover. The resolution of the MODIS is 500 m, which results in limitations when monitoring alpine terrain due to shadowed pixels (Hall et al. 2002). The forest coverage rate in Gansu is 10.42 % (Jia 2009), and the accuracy of MODIS snow products in forest could be a little lower than that in the other landscapes (Klein et al. 1998); therefore, the forest coverage has a certain influence on the accuracy of snow cover recognition from MODIS. We did not analyse several important snow cover factors, such as the snow water equivalent (SWE) and the number of snow cover days. Furthermore, the time series studied in this paper is relatively short. Thus, the snow cover variations in Gansu for a long time series and their responses to climate change must be further explored.

Acknowledgments This work is financially supported by a program from the National Nature Science Foundation (No. 41371391), a program from the National Key Technology Research and Development (No. 2012BAH28B02) and a program from the Specialized Research Fund for the Doctoral Program of Higher Education of China (No. 20120091110017). Also, this work was partially supported by the Collaborative Innovation Center of Novel Software Technology and Industrialization. The MODIS snow data used in this study are obtained from the National Snow and Ice Data Center (http://nsidc.org).

References

Armstrong RL, Brodzik MJ (2001) Recent Northern Hemisphere snow extent: a comparison of data derived from visible and microwave satellite sensors. Geophys Res Lett 28(19):3673–3676. doi:10.1029/2000GL012556

Barnett TP, Dümenil L, Schlese U, Roeckner E (1988) The effect of Eurasian snow cover on global climate. Science 239(4839):504–507. doi:10.1126/science.239.4839.504

Bavay M, Lehning M, Jonas T, Löwe H (2009) Simulations of future snow cover and discharge in alpine headwater catchments. Hydrol Process 23(1):95–108. doi:10.1002/hyp.7195

Biggs EM, Atkinson PM (2011) A characterization of climate variability and trends in hydrological extremes in the Severn Uplands. Int J Climatol 31(11):1634–1652. doi:10.1002/joc.2176

Bulygina ON, Groisman PY, Razuvaev VN, Korshunova NN (2011) Changes in snow cover characteristics over Northern Eurasia since 1966. Environ Res Lett 6(4):045204. doi:10.1088/1748-9326/6/4/045204

Cohen J, Rind D (1991) The effect of snow cover on the climate. J Clim 4(7):689–706. doi:10.1175/1520-0442(1991)004<0689:TEOSCO>2.0.CO;2

Dewey KF, Heim JR (1982) A digital archive of Northern Hemisphere snow cover, November 1966 through December 1980. Bull Am Meteorol Soc 63(10):1132–1141. doi:10.1175/1520-0477(1982)063<1132:ADAONH>2.0.CO;2

Farr TG, Rosen PA, Caro E, Crippen R, Duren R, Hensley S, Kobrick M, Paller M, Rodriguez E, Roth L, Seal D, Shaffer S, Shimada J, Umland J, Werner M, Oskin M, Burbank D, Alsdorf D (2007) The shuttle radar topography mission. Rev Geophys 45(2). doi:10.1029/2005RG000183

Feng SW (1989) Geography introduction in Gansu. Lanzhou Education Press, Lanzhou (in Chinese)

Foppa N, Seiz G (2012) Inter-annual variations of snow days over Switzerland from 2000–2010 derived from MODIS satellite data. Cryosphere 6(2):331–342. doi:10.5194/tc-6-331-2012

Frei A, Robinson DA (1999) Northern hemisphere snow extent: regional variability 1972–1994. Int J Climatol 19(14):1535–1560. doi:10.1175/1520-0442(1991)004<0689:TEOSCO>2.0.CO;2

Grody NC, Basist AN (1996) Global identification of snow cover using SSM/I measurements. IEEE Trans Geosci Remote 34(1):237–249. doi:10.1109/36.481908

Hall DK, Riggs GA (2007) Accuracy assessment of the MODIS snow products. Hydrol Process 21(12):1534–1547. doi:10.1002/hyp.6715

Hall DK, Riggs GA, Salomonson VV (1995) Development of methods for mapping global snow cover using moderate resolution imaging spectroradiometer data. Remote Sens Environ 54(2):127–140. doi:10.1016/0034-4257(95)00137-P

Hall DK, Riggs GA, Salomonson VV, DiGirolamo NE, Bayr KJ (2002) MODIS snow-cover products. Remote Sens Environ 83(1):181–194. doi:10.1016/S0034-4257(02)00095-0

Han LY, Sun LD, Zhang CJ, Guo AM (2011) The snow coverage change in eastern section of Qilian Mountain and its responding. J Arid Land Resour Environ 25(5):109–112 (in Chinese)

Huang XD, Zhang XT, Li X, Liang TG (2007) Accuracy analysis for MODIS snow products of MOD10A1 and MOD10A2 in Northern Xinjiang area. J Glaciol Geocryol l29(5):722–729, in Chinese

Jia ZB (2009) The 7th Chinese forest resource report. China Forestry Publishing House, Beijing, in Chinese

Ke CQ, Liu X (2014) MODIS-observed spatial and temporal variation in snow cover in Xinjiang, China. Clim Res 59(1):15–26. doi:10.3354/cr01206

Ke CQ, Yu T, Yu K, Tang GD, King L (2009) Snowfall trends and variability in Qinghai, China. Theor Appl Climatol 98(3–4):251–258. doi:10.1007/s00704-009-0105-1

Klein AG, Hall DK, Riggs GA (1998) Improving snow cover mapping in forests through the use of a canopy reflectance model. Hydrol Process 12(10–11):1723–1744. doi:10.1002/(SICI)1099-1085(199808/09)12:10/11<1723::AID-HYP691>3.0.CO;2-2

Liang TG, Huang XD, Wu CX, Liu XY, Li WL, Guo ZG, Ren JZ (2008) An application of MODIS data to snow cover monitoring in a pastoral area: a case study in Northern Xinjiang, China. Remote Sens Environ 112(4):1514–1526. doi:10.1016/j.rse.2007.06.001

Linde J, Grab S (2011) The changing trajectory of snow mapping. Prog Phys Geogr 35(2):139–160. doi:10.1177/0309133311399493

Luo F, Qi SZ, Xiao HL (2005) Landscape change and sandy desertification in arid areas: a case study in Zhangye Region of Gansu Province, China. Environ Geol 49(1):90–97. doi:10.1007/s00254-005-0062-7

Maskey S, Uhlenbrook S, Ojha S (2011) An analysis of snow cover changes in the Himalayan region using MODIS snow products and in-situ temperature data. Clim Chang 108(1–2):391–400. doi:10.1007/s10584-011-0181-y

Mazari N, Tekeli AE, Xie H, Sharif HO, Hassan AA (2013) Assessment of ice mapping system and moderate resolution imaging spectroradiometer snow cover maps over Colorado Plateau. J Appl Remote Sens 7(1):073540–073540. doi:10.1117/1.JRS.7.073540

Oguntunde PG, Friesen J, van de Giesen N, Savenije HH (2006) Hydroclimatology of the Volta River Basin in West Africa: trends and variability from 1901 to 2002. Phys Chem Earth 31(18):1180–1188. doi:10.1016/j.pce.2006.02.062

Parajka J, Pepe M, Rampini A, Rossi S, Blöschl G (2010) A regional snow-line method for estimating snow cover from MODIS during cloud cover. J Hydrol 381(3):203–212. doi:10.1016/j.jhydrol.2009.11.042

Paudel KP, Andersen P (2011) Monitoring snow cover variability in an agropastoral area in the Trans Himalayan region of Nepal using MODIS data with improved cloud removal methodology. Remote Sens Environ 115(5):1234–1246. doi:10.1016/j.rse.2011.01.006

Pu Z, Xu L (2009) MODIS/Terra observed snow cover over the Tibet Plateau: distribution, variation and possible connection with the East Asian Summer Monsoon (EASM). Theor Appl Climatol 97(3–4):265–278. doi:10.1007/s00704-008-0074-9

Pu Z, Xu L, Salomonson VV (2007) MODIS/Terra observed seasonal variations of snow cover over the Tibetan Plateau. Geophys Res Lett 34(6). doi:10.1029/2007GL029262

Ramsay BH (1998) The interactive multisensor snow and ice mapping system. Hydrol Process 12(10):1537–1546. doi:10.1002/(SICI)1099-1085(199808/09)12:10/11<1537::AID-HYP679>3.3.CO;2-1

Salomonson V, Appel I (2006) Development of the Aqua MODIS NDSI fractional snow cover algorithm and validation results. IEEE Trans Geosci Remote 44(7):1747–1756. doi:10.1109/TGRS.2006.876029

Shi Y, Shen Y, Kang E, Li D, Ding Y, Zhang G, Hu R (2007) Recent and future climate change in northwest China. Clim Chang 80(3–4):379–393. doi:10.1007/s10584-006-9121-7

Sönmez I, Tekeli AE, Erdi E (2014) Snow cover trend analysis using Interactive Multisensor Snow and Ice Mapping System data over Turkey. Int J Climatol 34(7):2349–2361. doi:10.1002/joc.3843

Tang Z, Wang J, Li H, Yan L (2013) Spatiotemporal changes of snow cover over the Tibetan plateau based on cloud-removed moderate resolution imaging spectroradiometer fractional snow cover product from 2001 to 2011. J Appl Remote Sens 7(1):073582–073582. doi:10.1117/1.JRS.7.073582

Wang X, Xie H, Liang T (2008) Evaluation of MODIS snow cover and cloud mask and its application in Northern Xinjiang, China. Remote Sens Environ 112(4):497–513. doi:10.1016/j.rse.2007.05.016

Wang W, Liang T, Huang X, Feng Q, Xie H, Liu X, Chen M, Wang X (2013) Early warning of snow-caused disasters in pastoral areas on Tibetan Plateau. Nat Hazard Earth Syst 13(6):1411–1425. doi:10.5194/nhess-13-1411-2013

Xia W, Xie H, Ke CQ (2014) Assessing trend and variation of Arctic sea ice extent during 1979–2012 from a latitude perspective of ice edge. Polar Res 33:21249. doi:10.3402/polar.v33.21249

Xie H, Liang T, Wang X (2009) Development and assessment of combined Terra and Aqua snow cover products in Colorado Plateau, USA and northern Xinjiang, China. J Appl Remote Sens 3(1):033559–033559. doi:10.1117/1.3265996

Zhou X, Xie H, Hendrickx JMH (2005) Statistical evaluation of remotely sensed snow-cover products with constraints from streamflow and SNOTEL measurements. Remote Sens Environ 94(2):214–231. doi:10.1016/j.rse.2004.10.007